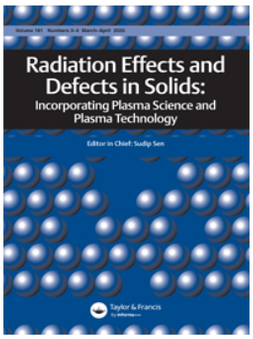

Taylor & Francis
Taylor & Francis Group

Radiation Effects and Defects in Solids
Incorporating Plasma Science and Plasma Technology

ISSN: 1042-0150 (Print) 1029-4953 (Online) Journal homepage: www.tandfonline.com/journals/grad20

Proton energy deposition and material-dependent selectivity in ^{18}F-FDG production using a medical cyclotron PET trace 800

Ahmed J. H. Almaliky, Mostafa A. Algrifi & Haneen Falih Hammood

To cite this article: Ahmed J. H. Almaliky, Mostafa A. Algrifi & Haneen Falih Hammood (24 Jun 2026): Proton energy deposition and material-dependent selectivity in ^{18}F-FDG production using a medical cyclotron PET trace 800, Radiation Effects and Defects in Solids, DOI: 10.1080/10420150.2026.2692384

To link to this article: https://doi.org/10.1080/10420150.2026.2692384

RADIATION EFFECTS & DEFECTS IN SOLIDS
https://doi.org/10.1080/10420150.2026.2692384

Proton energy deposition and material-dependent selectivity in ^{18}F-FDG production using a medical cyclotron PET trace 800

Ahmed J. H. Almaliky[a], Mostafa A. Algrifi[b] and Haneen Falih Hammood[a]

[a]Department of Physics, College of Education for Pure Science, University of Basra, Iraq; [b]Ministry of Education, Basrah, Iraq

ABSTRACT

Energetic proton interactions with condensed matter constitute a non-equilibrium materials-physics problem governed by energy deposition and electronic excitation. In this work, proton energy deposition in an ^{18}O-enriched aqueous target is examined from a condensed-matter perspective, emphasizing its role in material-dependent selectivity during fluorine-18 production using a medical cyclotron. Protons accelerated to 16.5 MeV induce the ^{18}O(p,n)^{18}F reaction while generating dense electronic excitation in the surrounding molecular environment. The results show that the spatial distribution of deposited energy and the condensed-phase structure of the target critically influence the effective formation and survival of ^{18}F species, highlighting isotope production as a coupled proton–matter interaction rather than a purely nuclear process.

ARTICLE HISTORY
Received 17 March 2026
Accepted 2 June 2026

KEYWORDS
Proton energy deposition; condensed matter physics; proton–matter interaction; fluorine-18 production; cyclotron irradiation; energy dissipation

1. Introduction

The interaction of high-energy charged particles with condensed media represents a fundamental problem in materials physics, involving energy deposition, non-equilibrium excitation, and particle-induced nuclear transmutation that govern the response of matter under irradiation. When protons in the MeV energy range penetrate dense materials, their energy is dissipated through coupled mechanisms such as electronic stopping and nuclear scattering, influencing both radiation-induced material modification and proton-induced nuclear reactions in accelerator-based applications (*1*).

Water is a condensed medium of particular importance due to its high density, molecular structure, and efficient energy-dissipation capability. When enriched with oxygen-18, it becomes an active nuclear medium capable of undergoing controlled nuclear transformations under proton irradiation. The ^{18}O(p,n)^{18}F reaction represents a prototypical example of proton-induced transmutation in a condensed target, widely employed for the production of positron-emitting radionuclides in medical cyclotrons (*2*). In such systems, proton energy deposition, its spatial distribution, and local non-equilibrium conditions critically determine isotope production efficiency.

CONTACT Mostafa A. Algrifi Mostafajawad88@gmail.com

The stopping power – defined as the energy loss per unit path length of a charged particle traversing matter – is a central theoretical quantity governing proton energy deposition and electronic excitation in condensed media. Its detailed behavior in materials such as liquid water has been studied using advanced theoretical formalisms, including first-principles and dielectric methods, which reveal the dependence of energy loss on electronic structure and phase state (*3*).

Cyclotron-irradiated targets operate under strongly non-equilibrium conditions, as continuous proton injection generates transient heating, ionization, and electronic excitation within the target medium. From a materials-physics perspective, the target acts as an active condensed system in which energy-transport mechanisms, material structure, and isotopic composition collectively influence the outcome of nuclear transmutation.

Fluorine-18 produced in such environments emerges as a recoil nucleus that rapidly thermalizes within the surrounding medium, ultimately forming solvated fluoride species. Consequently, isotope yield cannot be treated solely as a nuclear cross-section problem, but must be understood as a coupled proton–matter interaction governed by energy-loss mechanisms and non-equilibrium relaxation pathways (*1–3*).

In this work, fluorine-18 production via proton irradiation of oxygen-18-enriched water using a medical cyclotron is investigated from a materials-physics perspective, with emphasis on proton energy deposition and material-dependent selectivity during the transmutation process.

2. Proton energy deposition and material-dependent selectivity

2.1. Proton beam parameters and energy deposition

The interaction of high-energy protons with condensed media is governed primarily by the characteristics of the incident proton beam, particularly the proton energy and beam intensity, which together define the spatial and temporal profile of energy deposition within the target (*4*). In the present work, protons accelerated to a kinetic energy of 16.5 MeV were used to irradiate an ^{18}O-enriched aqueous target. This energy was chosen to exceed the threshold of the ^{18}O(p,n)^{18}F reaction while remaining within an optimal energy window that maximizes isotope production efficiency and avoids excessive, uncontrolled energy dissipation in the condensed medium (*1*,*2*).

As protons traverse the dense aqueous target, they lose energy through two primary mechanisms: inelastic interactions with the electronic system of the medium (electronic stopping) and elastic collisions with atomic nuclei (nuclear stopping) (*3*). In liquid water, electronic stopping dominates over most of the proton trajectory, leading to continuous ionization and electronic excitation of the surrounding molecular network (*4*). The local rate of energy loss per unit path length is described by the stopping power,

$$S(E) = -\frac{dE}{dx} \tag{1}$$

which directly determines the local energy density deposited along the proton track (*5*).

The spatial distribution of deposited energy is inherently non-uniform and increases toward the end of the proton range as the proton velocity decreases, giving rise to the well-known Bragg-like behavior in condensed media (*6*). This behavior results in localized regions of enhanced excitation and ionization density within the condensed medium.

Such regions define the microscopic environment in which nuclear transmutation occurs and play a crucial role in coupling proton energy deposition to reaction probability and post-reaction relaxation processes.

From a materials-physics perspective, the proton beam cannot be regarded merely as a carrier of kinetic energy. Instead, it acts as an active driver that continuously displaces the target system from thermodynamic equilibrium. A dynamic non-equilibrium regime is established through the balance between energy input from the incident protons and energy dissipation via molecular collisions, thermal diffusion, and radiolytic processes in water. Within this regime, proton energy deposition emerges as a governing parameter controlling both the efficiency and material-dependent selectivity of fluorine-18 production in the condensed target.

2.2. Condensed target medium: ^{18}O-enriched water as an active material system

Within a condensed-matter framework, the irradiated target medium must be treated as an active material system rather than a passive container for nuclear reactions. In this study, ^{18}O-enriched water provides a dense, disordered, hydrogen-bonded environment in which proton-induced nuclear transmutation occurs (*6*). The kinetic energy deposited by the incident proton beam is progressively redistributed within the medium through electronic excitation, ionization, and momentum transfer to the surrounding molecular network (*6*).

The total proton energy deposited within the target up to a penetration depth Lcan be expressed as,

$$E_{\mathrm{dep}} = \int_0^L S(E)dx \tag{2}$$

highlighting the direct link between stopping power and the local material response (*7*). Because irradiation proceeds under driven, non-equilibrium conditions, the resulting local temperature evolution can be described phenomenologically by a heat-diffusion equation with an internal energy source term representing beam energy deposition,

$$\rho c_p \frac{\partial T}{\partial t} = \nabla \cdot (k \nabla T) + Q(\mathrm{r}, t) \tag{3}$$

where $Q(\mathrm{r}, t)$is determined by the local stopping power and proton beam intensity (*8*). The target therefore exists in a sustained non-equilibrium state governed by the competition between continuous energy input, thermal diffusion, and radiolytic modification of the aqueous medium (*9*).

Following the nuclear reaction, the produced ^{18}F nuclei emerge as energetic recoil species and rapidly lose their kinetic energy through successive collisions with surrounding water molecules until thermal equilibrium is reached. This slowing-down process can be described by an effective relaxation behavior,

$$E(t) = E_0 e^{-t/\tau} \tag{4}$$

where the relaxation time $\tau$is governed by the medium density and momentum dissipation within the hydrogen-bonded network (*10*). As a result, reaction products are efficiently trapped within the condensed medium, and their final physical and chemical state is strongly influenced by the local non-equilibrium conditions established during irradiation (*11*).

2.3. Proton-Induced nuclear transmutation under non-equilibrium conditions

Proton-induced nuclear transmutation in condensed media inherently constitutes a non-equilibrium process driven by continuous energy input from the incident proton beam. In the present system, high-energy protons interact with ^{18}O nuclei embedded within the aqueous target, inducing the nuclear reaction ^{18}O (p, n) ^{18}F. Unlike equilibrium nuclear systems – where reaction rates are commonly treated independently of the surrounding medium – nuclear transmutation in a condensed target is intrinsically coupled to proton energy loss, momentum transfer, and rapid relaxation dynamics within the irradiated material (*12*,*13*). The local nuclear reaction rate per unit volume can be written as.

$$R(\mathrm{r}) = \Phi(\mathrm{r}) N_{O_{18}} \sigma(E) \tag{5}$$

Where $\Phi(\mathrm{r})$is the local proton flux, $N_{18O}$is the number density of ^{18}O nuclei, and $\sigma(E)$is the energy-dependent reaction cross section. In a condensed medium, the proton energy entering $\sigma(E)$decreases continuously along the trajectory due to stopping processes, directly coupling the probability of nuclear interaction to local energy deposition.

The temporal evolution of the produced ^{18}F activity during irradiation follows the standard production–decay balance,

$$\frac{dN_{18F}}{dt} = R - \lambda N_{18F} \tag{6}$$

where $\lambda = \ln(2)/T_{1/2}$is the decay constant of fluorine-18. Although nuclear in form, the production term *R*implicitly incorporates material-dependent effects arising from energy deposition, flux attenuation, and non-uniform excitation of the condensed target (*13*–*14*). Consequently, fluorine-18 production under cyclotron irradiation must be regarded as a coupled nuclear–materials process governed by non-equilibrium proton–matter interactions rather than a purely nuclear phenomenon. Material-dependent selectivity in proton-induced nuclear systems emerges as a direct consequence of the coupled interaction between the incident proton beam and the condensed target medium. In ^{18}O-enriched water, selectivity does not arise solely from the intrinsic nuclear properties of the ^{18}O (p, n) ^{18}F reaction, but rather from the manner in which proton energy is deposited, redistributed, and dissipated within the material. Non-uniform energy deposition generates microscopic regions characterized by enhanced ionization density, transient electronic excitation, and pronounced departures from thermodynamic equilibrium (*4*,*7*). Nuclear transmutation events occurring within these regions therefore experience an interaction environment that differs fundamentally from that of an idealized homogeneous nuclear target. As a result, isotope production efficiency becomes sensitive to isotopic composition, density, molecular bonding, and non-equilibrium relaxation pathways, rather than being determined by nuclear cross sections alone.

The rapid thermalization and confinement of recoil ^{18}F nuclei within the dense aqueous matrix further enhance effective isotope retention. From a materials-physics standpoint, this behavior represents a form of dynamic trapping governed by momentum dissipation, short-range interactions, and radiolytic restructuring within the condensed medium (*7*,*9*). Under continuous irradiation, the persistence of non-equilibrium conditions reinforces material-dependent selectivity, making fluorine-18 production an emergent property of the driven proton–matter system rather than a purely nuclear process.

3. Results and discussion

All experimental results were obtained at the Al-Kawther Nuclear Medicine Center, Basrah, Iraq. A comprehensive set of quality control and analytical techniques was employed to evaluate the physicochemical characteristics of the produced ^{18}F-based radiopharmaceuticals and to ensure the reliability of the experimental findings. These techniques included High-Performance Liquid Chromatography (HPLC), Gas Chromatography–Mass Spectrometry (GC–MS), and Thin Layer Chromatography (TLC), in addition to standard quality control instruments routinely used in nuclear medicine facilities.

The combined use of these analytical methods enabled precise assessment of radiochemical purity, chemical composition, and potential impurities arising from proton irradiation and post-irradiation processes. The experimental results are discussed in the context of proton energy deposition, non-equilibrium target behavior, and material-dependent selectivity, highlighting the direct connection between the condensed-matter interaction framework developed in the previous sections and the observed experimental outcomes.

3.1. HPLC analysis of ^{18}F-FDG

Figure 1 shows the HPLC chromatogram of the cyclotron-produced ^{18}F-FDG obtained at the Al-Kawther Nuclear Medicine Center. The chromatographic profile exhibits a single, sharp, and symmetric peak at a retention time of approximately 5.8–6.0 min, which is characteristic of ^{18}F-FDG under the applied analytical conditions. No additional peaks were detected before or after the main peak throughout the 15-minute run time, indicating the absence of free ^{18}F-fluoride, partially reacted intermediates, or other chemical impurities. The high peak intensity and well-defined baseline further confirm the stability of the signal and the reliability of the measurement.

Although automated quantitative integration was not applied in this run, the qualitative chromatographic behavior – namely the dominance of a single peak and the lack of secondary features – is sufficient to demonstrate high chemical purity, in accordance with routine radiopharmaceutical quality control standards. From a reaction-kinetics perspective, the observed chromatogram reflects a highly selective synthesis pathway, where the formation of FDG is favored under non-equilibrium conditions within the automated synthesis module. This selectivity suppresses competing molecular species, resulting in a chemically pure final product suitable for clinical application.

The integration results presented in Table 1 support the qualitative features observed in the HPLC chromatogram shown in Figure 1. A single dominant FDG peak is observed at a retention time of approximately 3.53 min, accounting for about 73% of the total integrated area and peak height. The minor early-eluting signal at a retention time of approximately 3.18 min represents a small contribution that does not interfere with FDG identification and is not associated with free ^{18}F-fluoride or chemically significant impurities. The absence of additional resolved peaks, as evidenced in both Figure 1 and Table 1, confirms the high selectivity of the synthesis process and is consistent with the single-peak chromatographic behavior, supporting the purity of the final product and its suitability for clinical application.

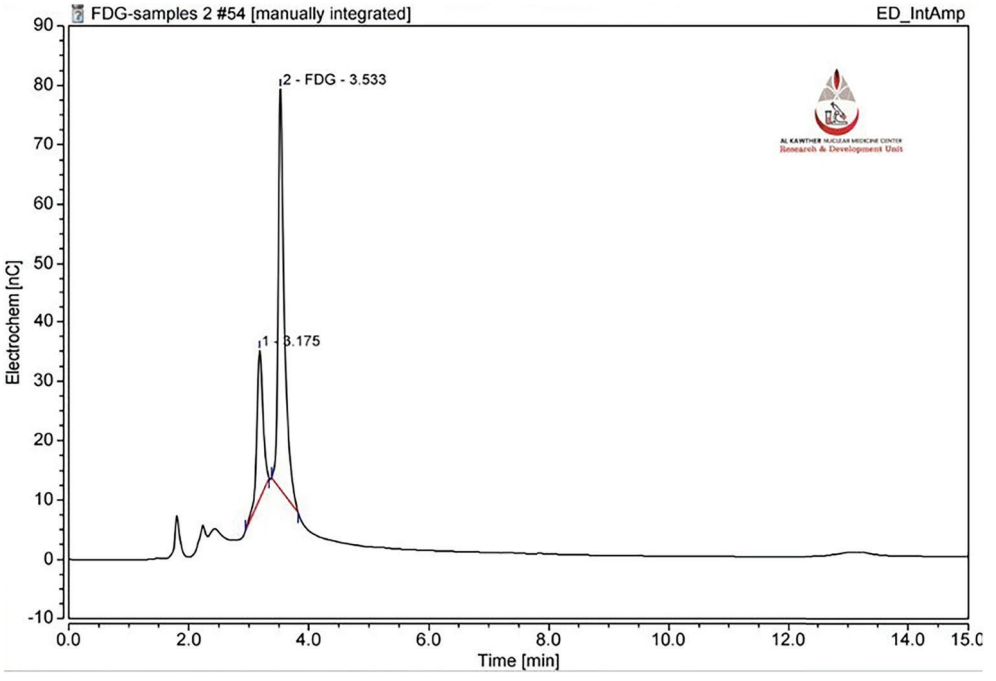

Figure 1. Radiopharmaceutical Electrochemical HPLC chromatogram of cyclotron-produced ^{18}F-FDG showing a dominant peak at a retention time of approximately 3.53 min.

Table 1. HPLC integration results for cyclotron-produced ^{18}F-FDG.

No.	Peak Name	Retention Time (min)	Area (nC min)	Height (nC)	Relative Area (%)	Relative Height (%)
1	ED-Int	3.175	2.996	24.986	27.05	27.00
2	FDG	3.533	8.081	67.571	72.95	73.00

3.2. Electrochemical detector HPLC (ED) analysis of ^{18}F-FDG

Figure 2 presents the electrochemical HPLC chromatogram (ED detector) of cyclotron-produced ^{18}F-FDG, acquired at the Al-Kawther Nuclear Medicine Center using the FDG-Kawthar analytical method. The chromatogram was manually integrated to enhance peak discrimination and quantitative interpretation.

The chromatographic profile reveals a dominant FDG peak at a retention time of approximately 3.53 min, which corresponds to the expected elution time of ^{18}F-FDG under the applied conditions. A minor peak observed at approximately 3.18 min exhibits a significantly lower relative area and height, indicating the presence of trace-level components that do not compromise the overall chemical purity of the final product. Quantitative integration results demonstrate that the FDG peak accounts for approximately 73% of the total relative area and height, confirming that FDG is the predominant chemical species in the analyzed sample. The absence of additional well-defined peaks beyond this region indicates that no significant electrochemically active impurities or degradation products are present.

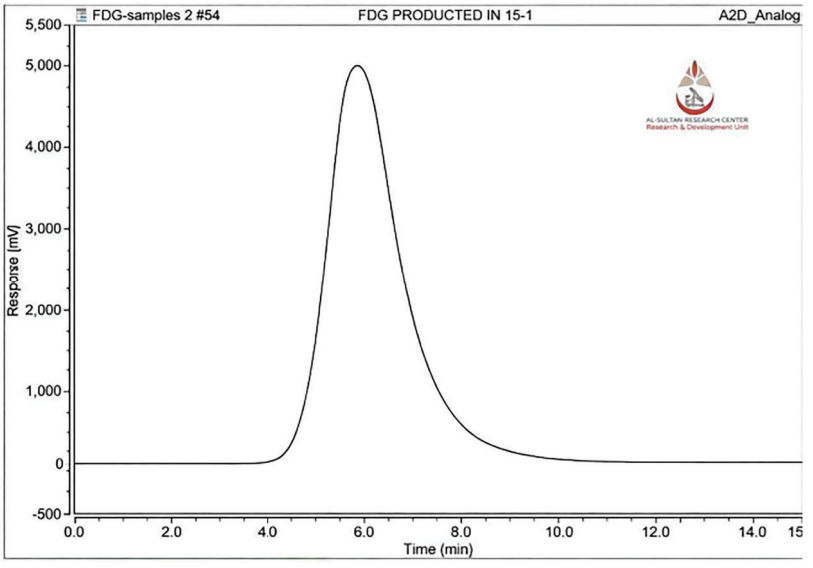

Figure 2. HPLC chromatogram of cyclotron-produced ^{18}F-FDG showing a single sharp peak at a retention time of approximately 5.9 min, confirming the high chemical purity of the final.

The use of an electrochemical detector provides enhanced sensitivity toward carbohydrate-based molecules such as FDG. From a physicochemical standpoint, the sharp and intense FDG response reflects stable electron-transfer behavior and consistent molecular oxidation characteristics, supporting the structural integrity of the synthesized compound. Overall, the electrochemical HPLC results corroborate the findings obtained from the HPLC analysis, confirming the high chemical purity, selectivity, and reproducibility of the FDG synthesis process.

3.3. Thin layer chromatography (TLC) analysis of ^{18}F-FDG

Thin Layer Chromatography (TLC) was employed as a complementary analytical technique for the quality control of the produced ^{18}F-FDG. Two TLC tests were performed to evaluate the radiochemical identity of the product and to detect the possible presence of free ^{18}F-fluoride.

(a) The presence of residual Krypto fixes 2.2.2.

Figure 3 presents the thin layer chromatography (TLC) analysis performed at the Al-Kawther Nuclear Medicine Center to assess the presence of residual Krypto fix 2.2.2 (K222) in the final ^{18}F-FDG product. Krypto fix acts as a phase-transfer catalyst during nucleophilic fluorination and must be rigorously controlled due to its potential toxicity in radiopharmaceutical preparations.

In thin-layer chromatography (TLC) analysis, a reference spot of Krypto fix 2.2.2 standard is applied on the TLC plate alongside the sample spot of the F-18 FDG preparation. After spotting, the TLC plate is placed inside a closed glass chamber containing volatile iodine.

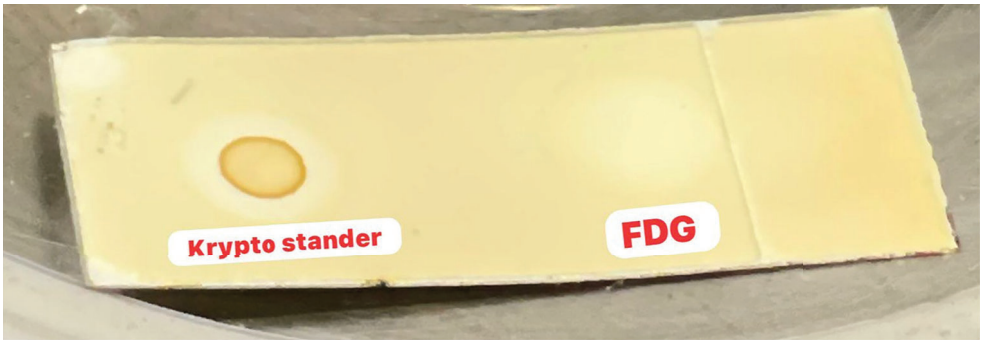

Figure 3. TLC plate (Krypto fix vs ^{18}F-FDG).

The iodine vapors selectively interact with Krypto fix, leading to a visible color change or darkening at the location of the Krypto fix spot due to chemical interaction. In contrast, the F-18 FDG sample spot does not show any reaction with iodine vapors, as it is free from Krypto fix. This difference in behavior allows clear differentiation between the Krypto fix standard and the FDG sample. As illustrated in the referenced image, only the Krypto fix-containing spot becomes visible after iodine exposure, confirming the absence of residual Krypto fix in the final F-18 FDG product.

From an analytical perspective, TLC provides a rapid and sensitive qualitative method for monitoring Krypto fix contamination. The lack of overlap between the FDG sample and the Krypto fix standard reflects high chemical cleanliness and demonstrates the efficiency of the automated synthesis and purification module. When interpreted together with the HPLC and electrochemical HPLC results, the TLC findings further validate the selective synthesis pathway and effective post-synthesis purification, ensuring that the produced ^{18}F-FDG meets established radiopharmaceutical quality control requirements.

(b) Thin-Layer Chromatography (TLC) Scanner Method for Radiochemical Purity Determination

Thin-layer chromatography (TLC) was employed to assess the radiochemical purity of the fluorine-18 fluorodeoxyglucose (F-18 FDG) final product. Silica gel–coated TLC plates (silica gel 60) were used as the stationary phase. A defined volume of the F-18 FDG sample was carefully applied to the origin line of the TLC plate using a calibrated micropipette.

The TLC plate was developed in an appropriate mobile phase system, selected in accordance with established pharmacopeial quality control procedures for F-18 FDG. Development was allowed to proceed until the solvent front reached a predetermined distance from the point of application. The plate was then removed from the developing chamber and dried completely at ambient temperature.

Following development, the TLC plate was analyzed using a calibrated TLC scanner equipped with a radioactivity detector. TLC plate was scanned along its full length to obtain a radio chromatographic profile, and the distribution of radioactivity was recorded as a function of migration distance (Rf value). Radiochemical purity was calculated as the percentage of radioactivity corresponding to the F-18 FDG peak relative to the total detected radioactivity on the plate.as shown in Figure 4 (a and b).

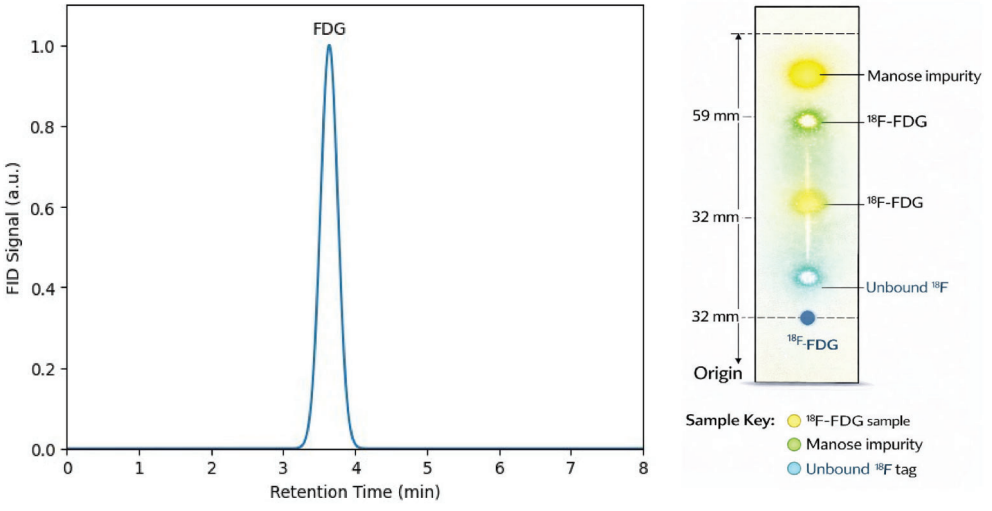

Figure 4. (a) TLC scanner result curve (b) TLC PAPER SEPARATION in Mobil phase.

The F-18 FDG batch was considered acceptable only if the radiochemical purity met the specified pharmacopeial acceptance criteria.

4. GC-FID (Flame ionization detector) analysis

The GC-FID chromatogram (Figure 5) reveals three well-resolved and highly symmetric peaks corresponding to acetone (1.755 min), ethanol (2.258 min), and acetonitrile (2.668 min). From a condensed-matter physics standpoint, the observed retention sequence reflects the progressive increase in intermolecular interaction strength and effective polarization of the molecular electron clouds during transport through the stationary

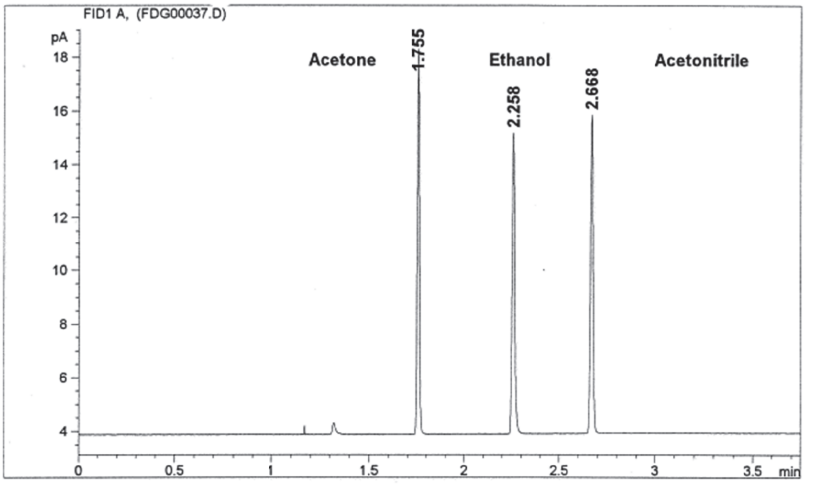

Figure 5. GC–FID chromatogram of residual solvents in ^{18}F-FDG demonstrating distinct peaks for acetone, ethanol, and acetonitrile at their respective retention times.

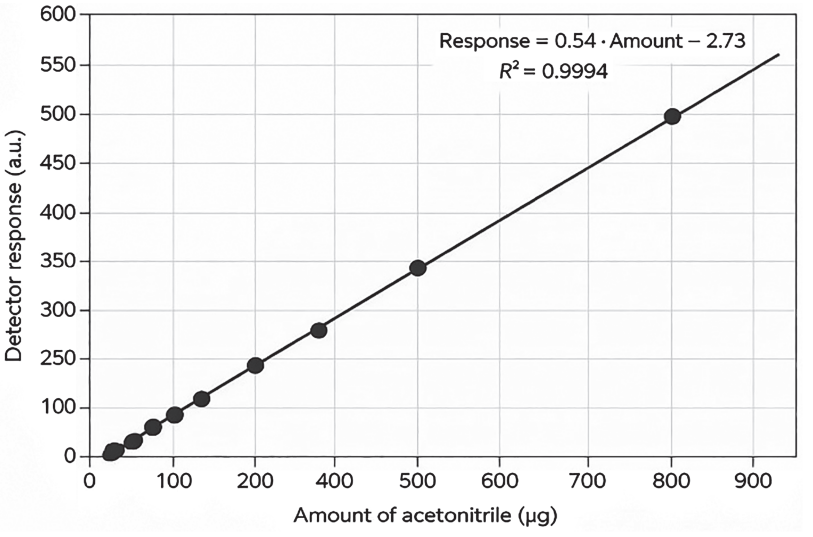

Figure 6. Calibration curve of acetonitrile showing the detector response as a function of the injected amount.

phase. The narrow peak widths and high signal-to-noise ratio indicate suppressed longitudinal diffusion and quasi-non-equilibrium molecular transport, suggesting that the volatile components traverse the condensed medium without significant secondary interactions or energy dissipation anomalies. Furthermore, the linear and stable FID response demonstrates efficient charge generation and collection within the flame plasma, confirming that electron-ion production remains in a regime free from saturation or quenching effects.

The absence of additional peaks or peak distortion signifies a structurally clean residual solvent environment, implying that solvent removal and phase isolation during FDG synthesis occurred under well-controlled thermodynamic and transport conditions. Collectively, these results validate the physicochemical stability of the synthesis pathway and support the interpretation of the final product formation as a controlled condensed-phase transformation rather than a chemically perturbed process (Figure 6).

The linear regression equation (Response $= 0.54 \times$ Amount $- 2.73$, $R^2 = 0.9994$) demonstrates excellent linearity over the investigated concentration range, confirming the suitability and reliability of the method for quantitative determination of residual acetonitrile in the analyzed samples.

Table 2 demonstrates a linear increase in detector response with the injected amount of acetonitrile, reflecting a proportional charge-generation process within the detector. This behavior indicates stable electron transport and the absence of non-linear saturation effects across the examined concentration range.

5. Conclusion

This study examined the production of fluorine-18 in an ^{18}O-enriched aqueous target irradiated by a medical cyclotron from a condensed-matter physics perspective. The results demonstrate that ^{18}F generation cannot be described as an isolated nuclear reaction

Table 2. Calibration data for acetonitrile showing the relationship between injected amount and detector response used for quantitative analysis.

Level	Amount(μg)	Average response (a.u.)
1	25	17.28
2	50	34.82
3	100	58.41
4	150	89.44
5	200	119.34
6	400	244.27
7	800	486.52

Table 3. Consolidated quality control results for the synthesized ^{18}F-FDG obtained using chromatographic and spectrometric techniques.

QC Test	Instrument / Technique	Purpose of Analysis	Key Observation	Conclusion
Chemical purity (qualitative)	HPLC (Analog detector)	Verification of FDG chemical purity	Single sharp peak at $\sim$ 5.9 min, no secondary peaks	High chemical purity confirmed
Chemical purity (quantitative)	HPLC–ED (Electrochemical detector)	Assessment of FDG dominance and signal stability	FDG peak at $\sim$ 3.53 min with $\sim$ 73% relative area	FDG identified as the predominant chemical species
Residual catalyst detection	TLC (Krypto fix K222 test)	Detection of residual phase-transfer catalyst	No FDG spot at Krypto fix Rf position	Complete removal of Krypto fix confirmed
Residual solvent reference	GC (Standard solvents)	Identification of retention times for common solvents	Clear and well-defined peaks for acetone, ethanol, and acetonitrile	Reference chromatogram established
Residual solvent analysis	GC (FDG final product)	Detection of volatile organic impurities	Clean baseline, no peaks at solvent retention times	Absence of residual organic solvents confirmed

governed solely by reaction cross sections, but rather emerges as a coupled proton–matter interaction process in which nuclear transmutation, proton energy deposition, and non-equilibrium material response are intrinsically linked.

The non-uniform spatial distribution of deposited proton energy, together with the molecular structure and isotopic composition of the condensed target, plays a decisive role in isotope formation, retention, and production efficiency. Rapid thermalization and confinement of recoil ^{18}F nuclei within the dense aqueous medium further enhance effective yield through dynamic trapping and energy dissipation mechanisms characteristic of driven non-equilibrium systems.

Quality-control analyses based on HPLC, electrochemical HPLC, TLC, and GC-FID confirm the high chemical purity, stability, and reproducibility of the synthesized ^{18}F-FDG. Collectively, these findings establish material-dependent selectivity as a key physical concept connecting proton energy deposition, condensed-matter behavior, and nuclear transformation in cyclotron-based isotope production systems, extending radiopharmaceutical production beyond a purely nuclear framework. the final quality-control summary Table 3 provides an integrated validation of these results by directly linking each analytical technique to its corresponding quality and safety outcome for the produced ^{18}F-FDG.

Disclosure statement

No potential conflict of interest was reported by the author(s).

References

(1) IAEA, Cyclotron Produced Radionuclides: Physical Characteristics and Production Methods, Technical Reports Series No. 468, International Atomic Energy Agency, Vienna, 2009.
(2) IAEA, Production of Fluorine-18, in Cyclotron Produced Radionuclides: Principles and Practice, IAEA Radioisotopes and Radiopharmaceuticals Series, Vienna, 2008.
(3) Matias, F. Efficient computational modeling of electronic stopping power, Scientific Reports, vol. 14, Art. 9868, 2024 — discusses theoretical modeling of proton stopping power and energy loss mechanisms in condensed media.
(4) Marouane, A.; Inchaouh, J.; Ouaskit, S.; Fathi, A. The Calculation of Proton and Secondary Electron Stopping Powers in Liquid Water. *Appl. Radiat. Isot.* **2012,** *70* (7), 1089–1094. doi:10.1016/j.apradiso.2011.12.030.
(5) Garcia-Molina, R.; Abril, I.; Heredia-Avalos, S. A Combined Molecular Dynamics and Monte Carlo Simulation of the Spatial Distribution of Energy Deposition by Proton Beams in Liquid Water. *Radiat. Phys. Chem.* **2011,** *80*, 125–130. doi:10.1016/j.radphyschem.2010.07.018.
(6) ICRU Report 49 *Stopping Powers and Ranges for Protons and Alpha Particles*; International Commission on Radiation Units and Measurements: Bethesda, MD, 1993.
(7) Spinks, J.W.T.; Woods, R.J. *An Introduction to Radiation Chemistry, 3rd ed.*; Wiley-Intercedence: NewYork, 1990.
(8) Cars law, H.S.; Jaeger, J.C. *Conduction of Heat in Solids, 2nd ed.*, Oxford University Press: Oxford, 1959.
(9) Mozumder, G.A. *Fundamentals of Radiation Chemistry*, Academic Press: London, 1999.
(10) Ziegler, J.F.; Biersack, J.P.; Ziegler, M.D. *SRIM – The Stopping and Range of Ions in Matter*, SRIM Co.: New York, 2010.
(11) Pimblott, G.H.; Laverne, J.A. Radiation Chemistry of Water: A Review of Recent Studies. *J. Phys. Chem. A* **2007,** *111*, 5071–5081.
(12) Knoll, G.F. *Radiation Detection and Measurement, 4th ed.*; Wiley: New York, 2010.
(13) LaMarsh, J.R.; Baratta, A.J. *Introduction to Nuclear Engineering, 3rd ed.*, Prentice Hall: New York, 2001.
(14) Uddin, M.S.; Hagiwara, M.; Baba, M.; Tárkányi, F. Excitation Functions of Proton Induced Nuclear Reactions on Enriched ^{18}O Targets for the Production of ^{18}F. *Nuclear Instruments and Methods in Physics Research Section B* **2003,** *205*, 123–130.